

# Equilibrium Contact Angle for Polymer/Polymer Interfaces

Elizabeth Vitt and Kenneth R. Shull\*

Department of Materials Science and Engineering,  
Northwestern University, Evanston, Illinois 60208-3108

Received November 28, 1994

Revised Manuscript Received May 23, 1995

## Introduction

The contact angle a fluid droplet makes with a given substrate is perhaps the most important parameter with regard to the wetting properties of the fluid/substrate system in question. Ideally, one would like to obtain a value of the equilibrium contact angle, which is a thermodynamically meaningful quantity. By balancing the surface and interfacial energies acting in the horizontal plane, one arrives at the familiar relationship derived very long ago by Young:

$$\gamma_A = \gamma_B \cos \theta + \gamma_{AB} \quad (1)$$

where  $\gamma_A$  and  $\gamma_B$  are the surface tensions of the A and B phases, and  $\gamma_{AB}$  is the interfacial tension between the A and B phases. The situation in real systems is complicated by contact angle hysteresis, with the equilibrium contact angle lying somewhere between the values obtained for advancing and receding droplets.

Contact angle hysteresis can be attributed to roughness or chemical heterogeneities in the surface with which the fluid is in contact.<sup>1</sup> The hysteresis is generally found to be a function of the size of the drop, so that advancing or receding angles will depend on the drop size. These effects can be described by an empirically defined "pseudo line tension".<sup>2,3</sup> In order to understand the significance of this quantity, it is useful to begin with a discussion of the true equilibrium line tension, which describes the energy per unit length of the three-phase contact line at the periphery of the droplet. This quantity plays an important role in a variety of processes, including the condensation of vapor onto a surface<sup>4</sup> and the separation of suspensions by flotation.<sup>5</sup> The effect of a finite line tension can be understood by analyzing the balance of forces acting at the three-phase contact line, as illustrated in Figure 1. We consider a fluid of phase B on a surface of phase A, against air. The existence of a positive line tension,  $\sigma$ , will provide a driving force for the drop to shrink in the lateral direction, thereby increasing the contact angle from the value predicted by eq 1. The net effect can be modeled as a force per unit length of magnitude  $\sigma/R$ , where  $R$  is the radius of curvature of the contact line. The force is directed toward the center of the droplet, and its inclusion gives the following "modified" Young equation:<sup>6</sup>

$$\gamma_A = \gamma_B \cos \theta + \gamma_{AB} + \sigma/R \quad (2)$$

The effect of the line tension on the measured contact angle can be obtained by rewriting eq 2 in the following form:

$$\cos \theta = \cos \theta_\infty - \sigma/\gamma_B R \quad (3)$$

with

$$\cos \theta_\infty = (\gamma_A - \gamma_{AB})/\gamma_B \quad (4)$$

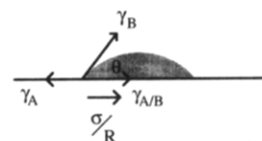


Figure 1. Schematic illustration of a fluid droplet on a solid substrate, showing the balance of forces acting on the contact line.

The effect of a positive line tension is therefore to increase the contact angle of sufficiently small droplets.

The theoretical prediction for  $\sigma$  is that its magnitude is quite small. From simple dimensional considerations Harkins obtained  $3 \times 10^{-6}$  dyn as an estimate for the line tension associated with the edge of an oil droplet on a water surface.<sup>7</sup> Line tension values of this magnitude are, in fact, consistent with flotation measurements.<sup>8</sup> However, eq 3 can typically only be used to fit the drop size dependence of the contact angles if unrealistically high values of the line tension are used, and for this region the term pseudo line tension applies. Positive and negative values of this quantity have been obtained by application of eq 3, with magnitudes on the order of 1 dyn obtained for millimeter-sized drops.<sup>2,3,9</sup> These values are orders of magnitude higher than the expected thermodynamic line tension and can most likely be attributed to the same effects which give rise to contact angle hysteresis, as described originally by Good and Koo.<sup>2</sup> Smaller drops give smaller values of the pseudo line tension, with magnitudes as low as  $10^{-3}$  dyn observed for drops with diameters less than 0.1 mm.<sup>3,10</sup> One explanation for this result is that the smallest drops have contact angles which more closely approximate the equilibrium values.

The aim of our work in this area is to develop a technique for measuring equilibrium contact angles for the interface between two polymeric materials. Toward this end, we have developed an ideal system for studying the contact angles of very small polymeric droplets. Consistency of our results with the measured surface energies, and the exceptionally low value of the pseudo line tension which we obtain ( $<10^{-4}$  dyn), indicates that the contact angle hysteresis in the system is very low and that the measured contact angle is very close to the equilibrium value. The utility of our technique is that it can be used to extract useful information concerning the equilibrium surface and interfacial energies of polymeric systems.

## Experimental Section

Our approach involves the use of atomic force microscopy to study the shapes of polymeric droplets which are glassy at room temperature. A glass-forming polymer is also used as the substrate in these experiments, giving well-defined values for  $\gamma_A$ ,  $\gamma_B$ , and  $\gamma_{AB}$ . Relatively high contact angles are obtained by using a dewetting liquid (poly(2-vinylpyridine)), which has a higher surface energy than the polymer used as the substrate (polystyrene, PS). A stable configuration is obtained by using polystyrene which has been end-grafted to a smooth silicon surface. Contact angle hysteresis on the grafted layer is potentially very low, because the polystyrene is a fluid at the temperature at which the droplets equilibrate (well above the glass transition temperature for both polymers).

The geometry of the samples before and after the dewetting process to form the individual droplets is shown in Figure 2. The grafted polystyrene used for the substrate layer was synthesized by terminating an anionic polymerization of deuterated polystyrene in THF with a large excess of [*p*-(chloromethyl)phenyl]trimethoxysilane.<sup>11</sup> (Other uses of this

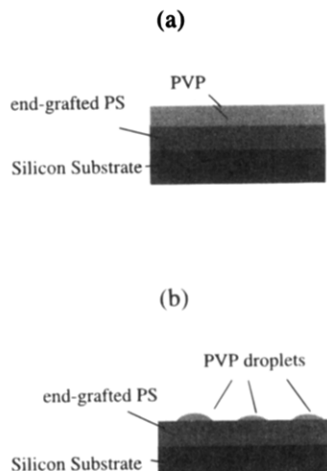


**Figure 2.** Sample geometry. Thin films of the PVP layer are cast on a grafted PS layer to produce samples as shown in part a. Part b shows the droplets which form when the samples are heated to temperatures above the glass transition temperature for PS and PVP.

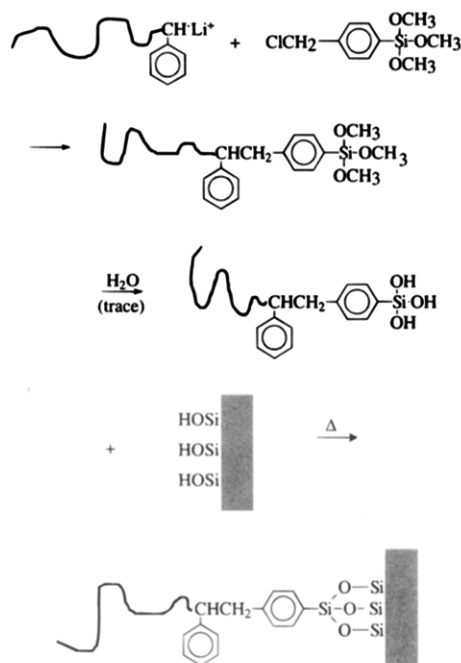


**Figure 3.** Scheme used to produce the end-grafted polystyrene layers.

polymer required that it be deuterated, but deuteration is not at all necessary for the purposes described here.) A layer of this polymer ( $M_w = 160\,000$ ,  $M_w/M_n < 1.05$ ) with a thickness of  $2000\text{--}3000\text{ \AA}$  was spun cast onto a smooth silicon wafer. The methoxysilyl groups readily hydrolyze to form silanol groups, which react with surface silanols on the silicon substrate during a subsequent annealing treatment in vacuum at  $170\text{ }^\circ\text{C}$ . The procedure is illustrated schematically in Figure 3. Ungrafted PS, along with any additional impurities (primarily from the large excess of methoxysilane used for the termination reaction), was removed by running a Soxhlet extraction in toluene for approximately 15 h.<sup>12</sup> Typical thicknesses for the grafted layers obtained in this way were  $200\text{ \AA}$ , as determined by ellipsometry. The grafted layers are similar to the ordered diblock copolymer layers which have been used as substrates in previous experiments.<sup>13,14</sup> One important difference is that our layers are truly grafted, and can not be significantly penetrated by the overlying polymer layer.

Thin films of poly(2-vinylpyridine) (PVP) were spun cast directly onto the grafted PS layers from solutions in *n*-butanol. The PVP used in our experiments was synthesized by anionic

**Table 1.** Measured Values of  $\gamma_{\text{PVP}}$

<i>M</i>	<i>T</i> ( $^\circ\text{C}$ )	$\gamma_{\text{PVP}}$ (dyn/cm)
6 300	137	36.2
6 300	147	35.3
6 300	166	33.6
45 000	184	35.0
45 000	194	34.4
45 000	201	34.0

polymerization in THF at  $-78\text{ }^\circ\text{C}$ , with secondary butyllithium as the initiator. This polymer has a weight-average molecular weight of 6300 as determined by light scattering, with a polydispersity index near 1.1 as determined by size-exclusion chromatography. These bilayer samples were then annealed in vacuum at various temperatures for 15 h in order to allow the dewetting to take place. The samples were rapidly quenched to room temperature by removing the samples from the annealing oven. The range of droplet sizes obtained during the annealing treatment was a function of the concentration of PVP in the solution from which the films were cast. Initial PVP layer thicknesses of approximately  $300\text{ \AA}$  gave a suitable range of droplet sizes. These films were imaged by optical microscopy and by atomic force microscopy (AFM). For the AFM measurements we used a Nanoscope II (Digital Instruments) equipped with pyramidal silicon nitride tips. Cantilevers with force constants of  $0.08$  and  $0.36\text{ N/m}$  were used in these experiments to verify that the detailed tip geometry did not influence our results.

The surface tension of the poly(2-vinylpyridine) used in these dewetting experiments was measured at a variety of different temperatures using a modification of the standard Wilhelmy method.<sup>15</sup> The measured values are listed in Table 1, along with values obtained for a monodisperse PVP sample with a higher molecular weight.

## Results

Optical micrographs of samples, viewed under reflected light after 15-h annealing treatments at  $130$ ,  $170$ , and  $200\text{ }^\circ\text{C}$ , are shown in Figure 4. The irregular shapes of the PVP droplets obtained after annealing at  $130\text{ }^\circ\text{C}$  indicate that equilibrium is clearly not obtained after annealing at this temperature. The projections of the droplets are less irregular for the anneal at  $170\text{ }^\circ\text{C}$  and are nearly circular after annealing at  $200\text{ }^\circ\text{C}$ . Our detailed analysis of the contact angles of the droplets relies on the existence of circular droplets. Our analysis here is therefore restricted to the samples annealed at  $170$  and  $200\text{ }^\circ\text{C}$ . While the contact angles for the droplets annealed at  $130\text{ }^\circ\text{C}$  are potentially very close to the equilibrium value, the shapes of the droplets are so irregular that it is very difficult to obtain a quantitative measurement of the contact angle.

An AFM view of the droplet structure obtained after an annealing treatment at  $170\text{ }^\circ\text{C}$  is shown in Figure 5a. Contact angles are obtained by profiling across the center of a droplet as shown in parts b and c of Figure 5. In principal, the contact angle can be obtained from the slope of the profile in the region very close to the contact line. However, for technical reasons and because the detailed shape of the droplet in the vicinity of the contact line can be distorted by local forces,<sup>13</sup> it is easier to obtain the contact angle from the macroscopic dimensions of the droplet. The contact angle is obtained from measurements of the drop height  $H$  and the drop radius  $R$  as follows:

$$\tan(\theta/2) = H/R \quad (5)$$

Equation 5 is valid for  $\theta < 90^\circ$ , and its use gives a "macroscopic" contact angle which is independent of the detailed shape of the drop in the region of the contact

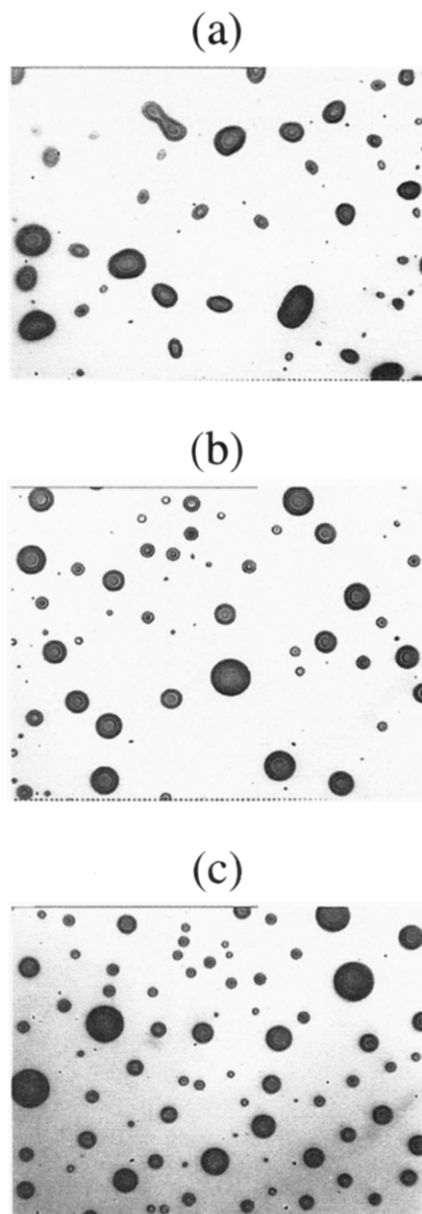


**Figure 4.** Optical micrographs of samples annealed for 15 h at 130 (a), 170 (b) and 200 °C (c).

line.<sup>6</sup> Use of this equation requires only that the edge of the drop be well-defined, so that an accurate value can be obtained for  $R$ . The estimated error in  $\theta$  associated with the accuracy in our measured values of  $H$  and  $R$  is 1°.

Values of  $H$  and  $R$  are obtained in the glassy state, after the samples have been quenched to room temperature. The volume contraction for polystyrene after a quench from 170 or 200 °C to room temperature is 7–8%.<sup>16</sup> We assume that the volume contraction of PVP is similar to that of PS and that the substrate constrains this contraction to be in the thickness direction. The actual values of  $H$  corresponding to the temperature at which the samples were annealed are therefore 7–8% higher than the values measured at room temperature, whereas the value of  $R$  is unchanged. We account for this correction when analyzing our data.

According to eq 3, a plot of  $\cos \theta$  as a function of  $1/R$  is expected to give a straight line with a slope of  $\sigma/\gamma_{\text{PVP}}$ . The results of such a plot are shown in Figure 6. The scatter in the data is noticeably larger for the 170 °C data than it is for the 200 °C data. We attribute this

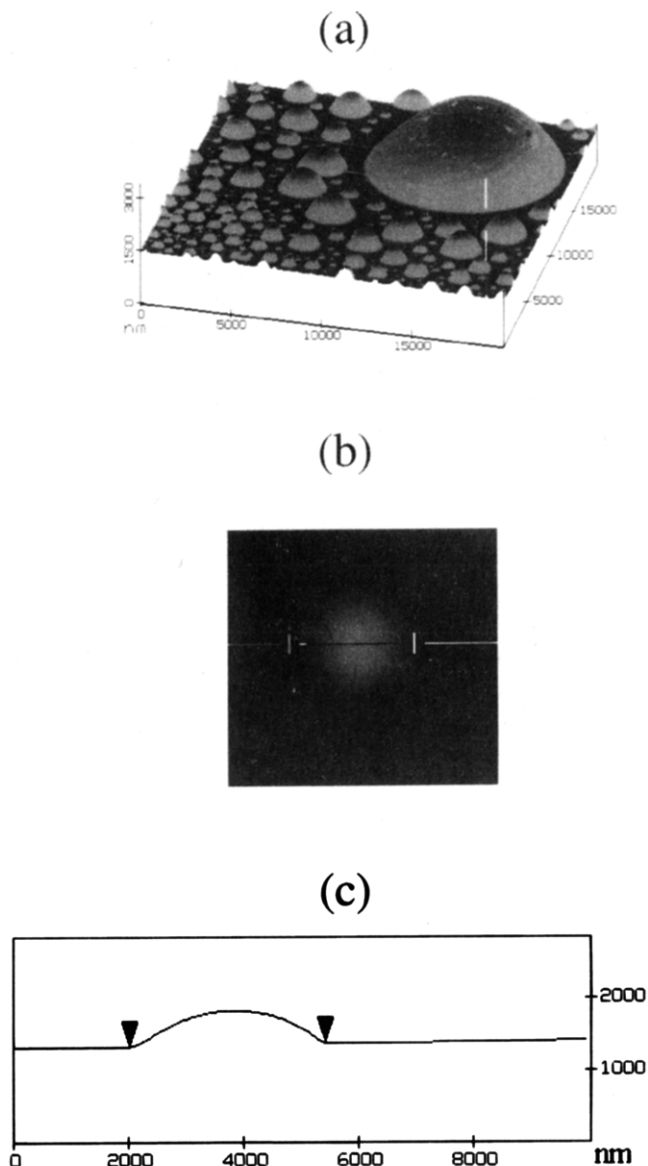


**Figure 5.** AFM images of the PVP droplets: (a) perspective showing the qualitative features of the droplet morphology; (b) a projection of an individual droplet; (c) line scan across the droplet from part b. The distance between the cursors is equal to  $2R$ , where  $R$  is the radius of the contact line. The height was determined in a similar fashion by placing one of the cursors at the top of the droplet.

result to the slightly more acircular drop shapes which are obtained at the lower annealing temperature. In both cases, the plots are flat, with no noticeable slope within the experimental scatter. This allows us to put a lower limit on the value of the pseudo line tension. The dashed line in Figure 6b has a slope corresponding to  $\sigma = 10^{-4}$  erg/cm ( $10^{-4}$  dyn) where we have used 31 dyn/cm for  $\gamma_{\text{PVP}}$ .

The low value of the pseudo line tension in our system is consistent with a very low contact angle hysteresis. One could argue, however, that the advancing angle could also be independent of drop size and still be quite different from the receding contact angle measured in our experiments. It is important, therefore, to verify the consistency of the measured contact angles with the PVP and PS surface tensions and with the PVP/PS interfacial tension. By neglecting the line tension contribution and by taking  $\gamma_A = \gamma_{\text{PS}}$  and  $\gamma_B = \gamma_{\text{PVP}}$ , we rewrite eq 1 as follows:

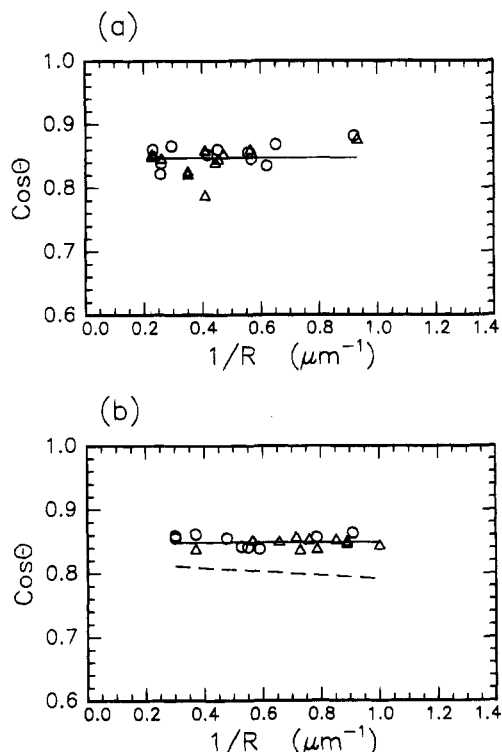


**Figure 6.** Cosine of the contact angle as a function of the drop size using cantilever tips with force constants of 0.08 (○) and 0.36 N/m (△): (a) annealed at 170 °C; (b) annealed at 200 °C.

$$\gamma_{pvp} = \frac{1}{\cos \theta}(\gamma_{ps} - \gamma_{ps/pvp}) = 1.17(\gamma_{ps} - \gamma_{ps/pvp}) \quad (6)$$

where we have used our experimentally determined value of 32° for  $\theta$ . Figure 7 shows the temperature dependence of  $\gamma_{pvp}$ . The values at 137, 147, and 166 °C are from Table 1 and were measured directly. The values at 170 and 200 °C were obtained from eq 6, using an estimated value for  $\gamma_{ps/pvp}$ , along with previously published values of  $\gamma_{ps}$ . From previous measurements of the surface tension of high molecular weight polystyrene,<sup>17</sup> we have  $\gamma_{ps} = 30.0$  dyn/cm at 170 °C and  $\gamma_{ps} = 28.1$  dyn/cm at 200 °C. The fact that the grafted polystyrene layer is deuterated in our case is of little consequence, because the surface energy difference between normal and deuterated polystyrene is less than 0.1 dyn/cm.<sup>18</sup>

Published values of  $\gamma_{ps/pvp}$  do not exist. As a rough estimate for its magnitude, we can begin with an expected form of the interfacial tension which is valid for homopolymers of infinite molecular weight:<sup>19</sup>

$$\gamma_{A/B} = a\varrho_0 k_B T (\chi/6)^{1/2} \quad (7)$$

where  $a$  is the statistical length of a polymer chain repeat unit,  $\varrho_0$  is the concentration of repeat units (the inverse of the repeat unit volume), and  $\chi$  is the Flory parameter characterizing the thermodynamic interaction between A and B repeat units. The  $\chi$  parameter for this system at 178 °C is 0.11, which when used with the known values for  $a$  and  $\varrho_0$ , gives 3.2 dyn/cm as an initial estimate for  $\gamma_{ps/pvp}$ .<sup>20</sup> Because the molecular weight of the PVP in our experiments is quite low (6300), we expect the interfacial tension to be somewhat lower than the value given by eq 6. We use 2.5 dyn/cm as an estimate which is consistent with the predictions

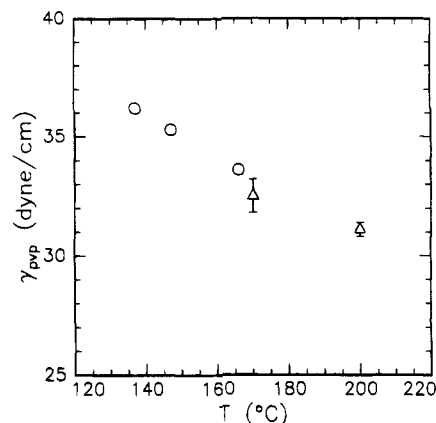


**Figure 7.** Poly(2-vinylpyridine) surface energy: measured (○); obtained from eq 6 (△).

of more detailed theories that include the molecular weight dependence.<sup>21,22</sup>

The magnitude of  $\gamma_{ps/pvp}$  is small compared to  $\gamma_{ps}$  or  $\gamma_{pvp}$ , so large relative errors in  $\gamma_{ps/pvp}$  do not significantly affect the comparison made in Figure 7. The error bars associated with the values obtained from eq 6 represent the error associated with our uncertainty in the contact angle. The measured contact angles are all within 1.5° of 32°. An error of 1.5° in the equilibrium contact angle corresponds to an error of 0.020 in  $1/\cos \theta$ , or an error of 0.57 dyn/cm in  $\gamma_{pvp}$ . The errors in  $\gamma_{ps}$  and  $\gamma_{ps/pvp}$  must, of course, be considered here as well. Within these errors, it is evident from Figure 7 that the measured and calculated values for  $\gamma_{pvp}$  are in good agreement, thereby providing a useful confirmation of the consistency of our data. Our assumption that the receding contact angles measured in these experiments are equal to the equilibrium values appears to be valid.

Our maximum value of  $10^{-4}$  dyn for the *pseudo* line tension is, of course, also a maximum value for the *equilibrium* line tension. When comparing this value to values obtained in other systems, one must consider system-specific effects. In our case, the line tension corresponds to that of an amorphous polymer on a grafted polymer layer. Distortions of the grafted chains in the vicinity of the contact line are therefore expected to give an additional contribution to the line tension which is not present when a truly solid substrate is used. One would not expect these extra contributions to the line tension to be dominant, however. Suppose, for example, that all of the polymer molecules within some distance  $\xi$  of the contact line contribute an extra energy of  $k_B T$  to the line tension. This contribution to the line tension from these distortions, referred to here as  $\sigma'$ , will then be given by the following expression:

$$\sigma' = k_B T \xi t / V \quad (8)$$

where  $t$  is the thickness of the grafted layer and  $V$  is the molecular volume of a grafted polymer chain. The distortion of the polymer brush acting as the substrate is suppressed over length scales which are significantly larger than the thickness of the film.<sup>23</sup> Taking  $\xi = t$  gives a contribution to the line tension of approximately  $10^{-6}$  dyn, which is similar in magnitude to the expected "nonpolymeric" contributions to the line tension.

## Summary

We have developed a methodology for studying equilibrium contact angles of polymeric fluids. Smooth

silicon substrates to which polymer molecules have been covalently grafted present a surface for which contact angle hysteresis appears to be very small, presumably due to the fluid character of the grafted polymer layer. This conclusion is based on the negligible drop size dependence of the contact angle and on the agreement with contact angles predicted from the surface and interfacial energies.

**Acknowledgment.** This work was supported by the National Science Foundation, through a Young Investigator Award to K.R.S. and through a summer internship to E.V. The authors thank Dr. B. B. Sauer of Du Pont for the measurements of the PVP surface energy.

## References and Notes

- (1) *Wettability and Contact Angles*; Johnson, R. E., Dettre, R. H., Eds.; Wiley: New York, 1969.
- (2) Good, R. J.; Koo, M. N. *J. Colloid Interface Sci.* **1979**, *71*, 283.
- (3) Drelich, J.; Miller, J. D.; Hupka, J. *J. Colloid Interface Sci.* **1993**, *155*, 379.
- (4) Mederos, L.; Quintana, A.; Navascués, G. *J. Appl. Phys.* **1985**, *57*, 559.
- (5) Schulze, H. J. *Physico-chemical Elementary Processes in Flotation*; Elsevier: Amsterdam, The Netherlands, 1984.
- (6) Pethica, B. A. *J. Colloid Interface Sci.* **1977**, *62*, 567.
- (7) Harkins, W. D. *J. Chem. Phys.* **1937**, *5*, 135.
- (8) Scheludko, A.; Toshev, B. V.; Bojadjev, D. T. *J. Chem. Soc., Faraday Trans. 1* **1976**, *72*, 2815.
- (9) Gaydos, J.; Neumann, A. W. *J. Colloid Interface Sci.* **1987**, *120*, 76.
- (10) Wallace, J. A.; Schurch, S. *Colloids Surf.* **1990**, *43*, 207.
- (11) Long, T. E.; Kelts, L. W.; Turner, S. R.; Wesson, J. A.; Mourey, T. H. *Macromolecules* **1991**, *24*, 1431.
- (12) The trimethoxysilyl end groups used to graft the polystyrene molecules to the silicon substrate can also react with one another to form larger polymer aggregates. Because of the steric hindrance of large polystyrene molecules, only starlike aggregates are formed. Grafting of these aggregates to the silicon surface can also take place and will affect the spatial distribution of grafting sites. The character of the surface with which the PVP is in contact is not expected to be significantly affected by this spatial distribution, however.
- (13) Leibler, L.; Ajdari, A.; Mourran, A.; Coulon, G.; Chatenay, D. In *Ordering in Macromolecular Systems*; Teramoto, A., Norisuje, M. K. T., Eds.; Springer-Verlag: Berlin, 1994; p 301.
- (14) Liu, M.; Rafailovich, M. H.; Sokolov, J.; Schwarz, S. A.; Zhong, X.; Eisenberg, A.; Kramer, E. J.; Sauer, B. B.; Satija, S. *Phys. Rev. Lett.* **1994**, *73*, 440.
- (15) Sauer, B. B.; DiPaolo, N. V. *J. Colloid Interface Sci.* **1991**, *144*, 527.
- (16) Hellwege, K. H.; Knappe, W.; Lehmann, P. *Kolloid Z.* **1963**, *183*, 110.
- (17) Dee, G. T.; Sauer, B. B. *J. Colloid Interface Sci.* **1992**, *152*, 85.
- (18) Jones, R. A. L.; Kramer, E. J.; Rafailovich, M. H.; Sokolov, J.; Schwarz, S. A. *Phys. Rev. Lett.* **1989**, *62*, 280.
- (19) Helfand, E.; Tagami, Y. *Polym. Lett.* **1971**, *9*, 741.
- (20) Shull, K. R.; Kramer, E. J.; Hadziioannou, G.; Tang, W. *Macromolecules* **1990**, *23*, 4780.
- (21) Tang, H.; Freed, K. F. *J. Chem. Phys.* **1991**, *94*, 6307.
- (22) Shull, K. R. *Macromolecules* **1993**, *26*, 2346.
- (23) Fredrickson, G. H.; Ajdari, A.; Leibler, L.; Carton, J.-P. *Macromolecules* **1992**, *25*, 2882.

MA946358V